



computational proteomics

Laboratory for Computational Proteomics

www.FenyoLab.org

E-mail: Info@FenyoLab.org

Facebook: [*NYUMC Computational Proteomics Laboratory*](#)

Twitter: [*@CompProteomics*](#)

Radial velocities of ejected ions: implications for the mechanisms of molecular ion formation in plasma desorption mass spectrometry of biomolecules

P Demirev, G Brinkmalm, D Fenyo, P Håkansson and B U R Sundqvist

*Division of Ion Physics, Department of Radiation Sciences, Uppsala University,
Box 535, Uppsala S-75121 (Sweden)*

(Received 17 April 1991)

ABSTRACT

Experimental data are presented on the initial radial velocity distributions of different types of secondary molecular ions, M^+ , $[M + H]^+$ and $[M + Na]^+$, ejected from biomolecular samples. An incident beam of 48 MeV $^{127}I^{11+}$ ions was employed to generate the secondary ions. Measurements were carried out in a reflectron time-of-flight mass spectrometer by monitoring the secondary ion yield as a function of electrostatic deflection in a direction perpendicular to the target surface normal. The data are interpreted in terms of current models describing the ejection process in plasma desorption mass spectrometry.

INTRODUCTION

Plasma desorption mass spectrometry (PDMS) exploits the phenomenon of sputtering of biomolecules following impact by fast (velocity greater than Bohr velocity) multiply charged atomic ions [1,2]. The mechanism of this desorption phenomenon (also termed “electronic” sputtering [3,4]) has not yet been completely elucidated [2–6]. Various aspects of the desorption process, e.g. energy deposition, energy conversion and energy transport, have been incorporated into theoretical models, including the “popcorn” and the “pressure pulse” models [7,8]. Neither of these models specifically addresses the charge state of the ejected particles. Sputtering experiments from biomolecular solids have demonstrated that 10^3 times more neutral intact molecules are ejected per primary particle compared with positive (10^4 for negative) molecular ions (for the amino acid leucine for example [9]). It is the ionic species which are observed directly by PDMS and are significant for its analytical applications.

There are two major types of molecular ion formed in PDMS as well as in all other desorption ionization techniques. These are the more rarely observed odd-electron radical ions of the type M^{\pm} and the more frequently found even-electron protonated/deprotonated $[M \mp H]^{\mp}$ molecules or adducts of

neutral sample molecules with one or more cations (most often alkali metal) or anions. Depending on the type of molecule and the target preparation technique employed, multiply charged molecular ions, owing to the attachment of more than one proton to the neutral molecule, are also observed in PDMS. Gas-phase ions, formed as a result of clustering of several neutral molecules (up to 23 for valine for example [3]) and a cation can also be detected, depending on the nature of the sample molecules.

Several points have to be addressed in a study of the ionization mechanism in PDMS. These include the region where the ionization step takes place—whether it is a gas-phase process or a surface and bulk process and accordingly whether it precedes or follows the ejection step. We have recently investigated the mechanism of formation of alkali metal cation adducts in PDMS of biomolecules [10]. To this end, the initial radial velocity distribution of the ejected secondary ions [11–13] was employed for probing the cationization process. We have demonstrated that alkali cation attachment to neutral biomolecules occurs at an early stage of the desorption event and precedes molecular ion ejection into the gas phase.

In the present study the radial velocity distribution for different types of biomolecular ions, M^+ , $[M + H]^+$ and $[M + Na]^+$, has been determined for the first time with a reflectron time-of-flight (TOF) spectrometer. Distributions for radical (odd-electron) molecular ions of the type M^+ , for which there are no previously available data, are compared with the data for even-electron molecular ions. The results are interpreted in terms of current models of ion ejection from biomolecular samples in plasma desorption mass spectrometry, addressing the issues listed above.

EXPERIMENTAL

All measurements on the initial radial velocity distribution of sputtered secondary ions were performed using a reflectron TOF spectrometer (Fig. 1) which has been described in detail elsewhere [14]. The improved mass resolution of the reflectron allowed accurate determination of the masses of the observed ions and unambiguous differentiation between species similar in mass such as radical and protonated molecular ions. An added advantage of the reflectron is that the influence of neutrals, formed as a result of metastable decomposition in the first field-free region, is avoided. Primary 48 MeV $^{127}\text{I}^{11+}$ ions from the Uppsala EN tandem accelerator bombarded the target from the front at a 45° angle of incidence. Initially accelerated positive secondary ions were deflected by means of a set of deflection plates in the plane of the incoming ion beam and the optical axis (z direction) of the spectrometer, perpendicular to the target normal (direction x , Fig. 1). The voltage V_1 on the set of y -deflection plates was optimized for the highest low mass secondary ion

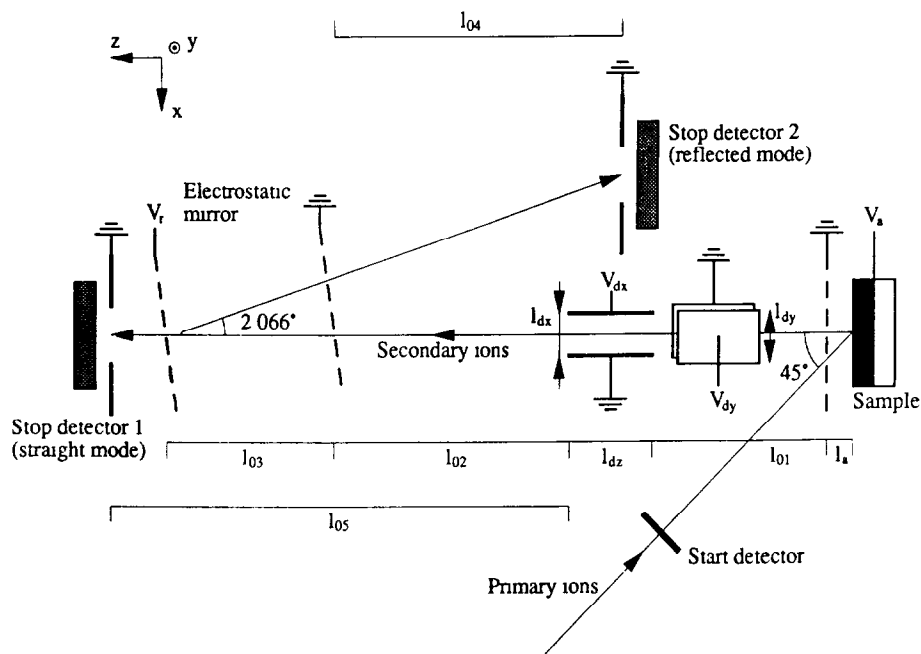


Fig 1 Schematics of the reflectron time-of-flight mass spectrometer

yield from each individual sample in order to compensate for an eventual non-parallel arrangement between different surfaces (e.g. target, detector and entrance grid), perpendicular to the ion optical axis. The V_y value was kept constant during the experiment. The yield of positive secondary ions as a function of the x -deflection voltage (V_x) was monitored with standard PDMS TOF ion-counting electronics. The v_x velocity component of the secondary ions in this paper is referred to as radial velocity. The ion accelerating voltage (V_a) was +15 kV and the mirror voltage (V_r) in the reflection mode was +15.8 kV. Between 2.5×10^5 (for ergosterol), 5×10^5 (for leu-enkephalin), 10^6 (for renin substrate) and 2×10^6 (for chlorophyll B) start count events were accumulated for each measurement point with an intensity of the primary beam between 1500 and 2500 ions s^{-1} .

Initial radial velocity distributions were obtained from the secondary ion yield as a function of V_x , measured both in the straight mode (with the mirror voltage off) and in the reflected mode. Use of a reflectron for radial velocity distribution studies is possible since the reflectron ion mirror compensates only for the axial energy distribution of the secondary ions. The procedure for conversion to radial velocity distribution has been described previously [13]. The explicit formulae for the case of the reflectron TOF spectrometer (assuming that the initial axial kinetic energy of the ions is small compared with the

acceleration energy) are the following For the straight mode

$$v_{0x}^{\text{straight}} = \left(\frac{|q|}{2m} \right)^{1/2} \frac{q}{|q|} \frac{V_{dx} - V_{0d}}{V_a^{1/2}} \frac{l_{dz} + \Delta l_{dz}}{l_{dx}} \frac{\frac{1}{2}l_{dz} + l_{05}}{2l_a + l_{01} + l_{dz} + l_{05}}$$

and for the reflected mode

$$v_{0x}^{\text{reflected}} = \left(\frac{|q|}{2m} \right)^{1/2} \frac{q}{|q|} \frac{V_{dx} - V_{0d}}{V_a^{1/2}} \frac{l_{dz} + \Delta l_{dz}}{l_{dx}} \frac{\frac{1}{2}l_{dz} + l_{02} + 2l_{03}(V_a/V_r) + l_{04}}{2l_a + l_{01} + l_{dz} + l_{02} + 2l_{03}(V_a/V_r) + l_{04}}$$

The different parameters in these equations are defined in Fig 1 V_{0d} is the deflection voltage needed to steer an ion with zero initial radial velocity v_v into the centre of the stop detector, Δl_{dz} is the first-order correction to the finite length of the deflection plates, m and q are the mass and charge of the secondary ion respectively The specific values are $l_a = 5$ mm, $l_{dx} = 14$ mm, $l_{dy} = 16$ mm, $l_{dz} = 24$ mm, $\Delta l_{dz} = 10$ mm, $l_{01} = 291$, $l_{02} = 370$, $l_{03} = 289$, $l_{04} = 433$, $l_{05} = 673$

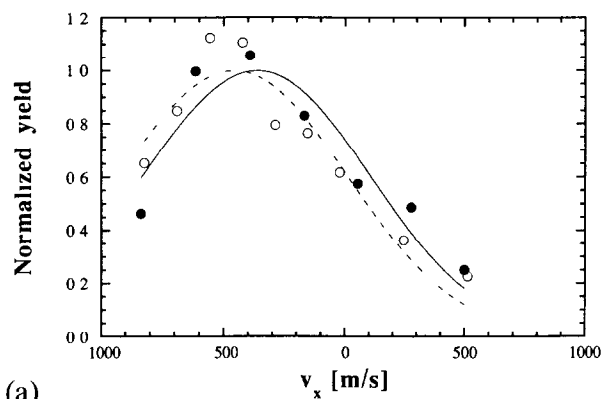
Commercially available samples (Sigma) were used without further purification Samples were prepared according to standard procedures The peptides, leu-enkephalin (mol wt 555) and renin substrate (RS, mol wt 1801), were dissolved in a mixture of 80% acetic acid and 20% trifluoroacetic acid at a concentration of $3 \mu\text{g} \mu\text{l}^{-1}$ and $9 \mu\text{g} \mu\text{l}^{-1}$ respectively A trace amount of NaI was added to the leu-enkephalin solution Ergosterol (mol wt 396) was dissolved in pyridine at a concentration of $3 \mu\text{g} \mu\text{l}^{-1}$ Chlorophyll B (mol wt 907.5) was dissolved in chloroform Solutions of ergosterol and leu-enkephalin ($30 \mu\text{l}$) were electrosprayed on a stainless steel backing RS was adsorbed from the solution onto a nitrocellulose layer that had been electrosprayed onto a steel backing Chlorophyll B was deposited on a steel backing by the spin-coating technique

RESULTS

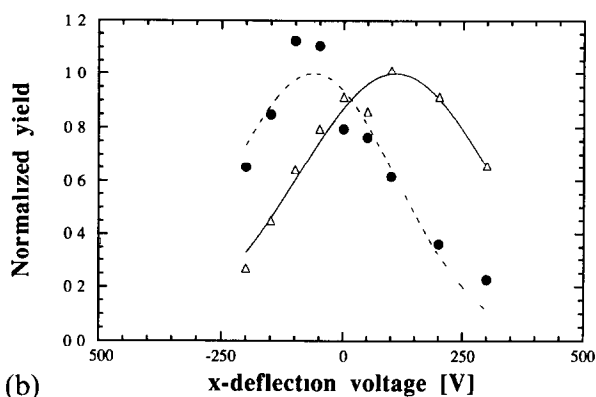
We studied samples that gave different types of molecular ions in their PD mass spectra The yields (number of molecular ions per primary ion) were also different for different samples, which is reflected in the different number of start events required to obtain adequate statistics (see Experimental section above) The peptides leu-enkephalin and RS form stable protonated $[M + H]^+$ and cationized $[M + Na]^+$ quasi-molecular ion species Peak corresponding to the $[2M + 3Na - 2H]^+$ singly charged dimer ion and $[M + 2Na - H]^+$ were also observed in the leu-enkephalin PD mass spectrum The chlorophyll B sample contained two components as shown by its PD mass spectrum the original compound and its oxidized form which gave a molecular ion peak 16u above the molecular ion corresponding to chlorophyll B The molecular ion peaks of both components had rather low

intensity Comparing their isotopic distributions we judge that the types of molecular ion formed for both chlorophyll B and its oxidized form are M^+ and $[M + H]^+$ On the basis of the oxidized component, which gave better resolved isotope peaks, we estimated that the M^+ was at least 60% of the total molecular ion signal In order to obtain better statistics in the radial velocity distribution the signals from both M^+ and $[M + H]^+$ molecular ions of oxidized chlorophyll B were integrated and reported in the results below We also did an independent study of ergosterol, which gave an abundant ion signal corresponding only to the radical molecular ion M^+ , in order to investigate the radial velocity distribution of odd-electron molecular ions without any interference

The possibility of employing a reflectron TOF spectrometer in order to estimate initial radial velocity distribution for desorbed secondary ions is demonstrated in Fig 2(a) in which the radial velocity distribution for a peptide, RS, measured both in the straight and the reflected mode, is presented In both straight and reflected modes there is a close overlap between the distributions As is well established by now [10–13,15], there is a shift between the yield distribution as a function of V_x for lower mass secondary ions (e.g. Na^+ , K^+ , Cs^+ , and fragments such as CH_3^+ , $C_2H_3^+$ etc) and higher mass quasi-molecular ($[M + H]^+$ and $[M + Alk]^+$) ions (Fig 2(b)) This shift has been observed in the reflection mode for the different types of molecular and cluster ions from leu-enkephalin (Fig 3) The shift is due to the directional correlation effect, observed as an ejection of higher molecular weight compounds preferentially at an angle away from the surface normal The angle of ejection for these compounds is correlated with the direction of the incoming ions [12,15] By contrast, the lower mass ions display ejection angle distributions which are symmetric about the surface normal, independent of the incidence angle The correlation effect, resulting from the non-diffusive momentum transfer from the expanding track core to the desorbed biomolecules, is predicted in the pressure pulse description of the ejection [9] A thermal mechanism of molecular ion evaporation would result in a distribution symmetric about the surface normal The directional correlation effect has also been demonstrated in molecular dynamics simulations of the phenomenon of electronic sputtering from biomolecules [16] The data on the radial velocity distribution of the molecular ion M^+ of ergosterol are given in Fig 4 The zero on the velocity scale corresponds to the centroid of the distribution of $C_2H_3^+$ fragment ions There is a noticeable shift between the centroids of the radial velocity distributions of M^+ and lower mass fragment ions A similar shift is observed for the molecular ion (in which 60% of the signal is due to M^+) of oxidized chlorophyll B (Fig 5) These data demonstrate convincingly that the directional correlation effect is observed for radical type molecular ions as well, similarly to protonated and cationized molecular ions (Figs 2 and 3)



(a)



(b)

Fig 2 (a) Radial velocity distribution of the renin substrate $[M + H]^+$ molecular ion in the straight (\bullet) and reflected (\circ) mode. The data points have been fitted with a gaussian curve. (b) Secondary ion yield distribution in the reflected mode as a function of x -deflection voltage for $[M + H]^+$ (\bullet) and lower mass fragment, e.g. $C_2H_3^+$ (Δ) for renin substrate sample. The data points have been fitted with a gaussian curve.

DISCUSSION

Several ionization mechanisms for PD have been discussed [1,2,17–20]. Early on it was suggested [17] that electron or proton transfer reactions and ion/dipole attachment are the basic processes of ionization of neutral molecules in PDMS. The ionization step should occur either in the gas phase or on the surface, as has been postulated [18]. The selvedge concept—the existence of a dynamic region on or above the target surface, where extensive mixing occurs—has been introduced for generating a unified description of different desorption/ionization phenomena, including laser desorption and secondary ion mass spectrometry (SIMS) [19]. There have been suggestions that a chemical ionization type mechanism, involving ion/molecule reactions

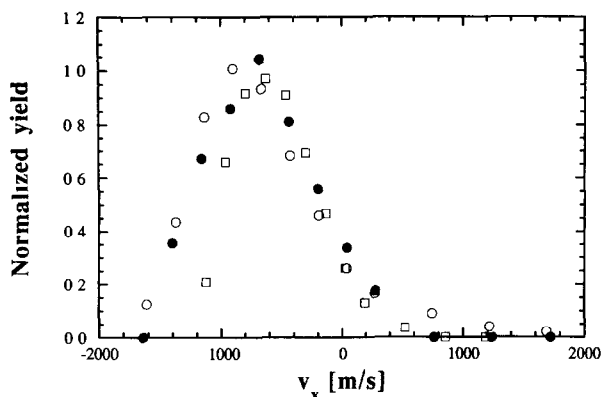


Fig 3 Radial velocity distribution for leu-enkephalin in the reflected mode ●, $[M + H]^+$, ○, $[M + Na]^+$, □, $[2M + 3Na - H]^+$ (Zero on the velocity axis corresponds to the centroid of the distribution of low mass ions, $C_2H_3^+$)

in the selvedge, may also result in protonated and/or cationized molecular ion species [19,20] Another idea involves the opposite process, uncluster dissociation reactions in the selvedge, leading to molecular ion formation [2] Macfarlane et al [21] have more recently elaborated on that process, putting forward a mechanism that includes ion pair formation in the condensed phase, and ejection and subsequent dissociation via different charge competing pathways Neither of these proposed mechanisms has been tested experimentally and verified rigorously until now

PDMS studies on Langmuir-Blodgett films of fatty acids demonstrated that molecular ions may originate not only from the surface but also from the

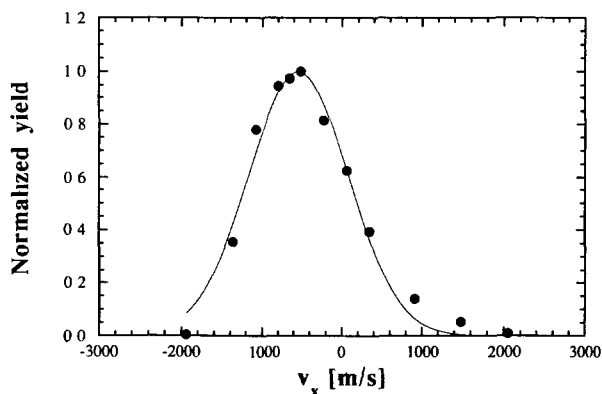


Fig 4 Radial velocity distribution for the ergosterol molecular ion M^+ in the reflected mode (zero on the velocity axis corresponds to the centroid of the distribution of low mass ions, $C_2H_3^+$) The data points have been fitted with a gaussian curve

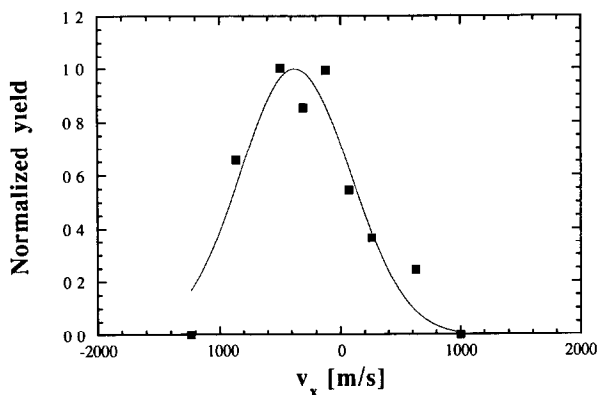


Fig 5 Radial velocity distribution for both M^+ and $[M + H]^+$ molecular ions of the oxidized component of chlorophyll B in the reflected mode (zero on the velocity axis corresponds to the centroid of the distribution of low mass ions, $C_2H_3^+$) The data points have been fitted with a gaussian curve

bulk [22,23] Ions from molecular layers 200 Å beneath the sample surface have been detected. These experiments indicate that ionization in PDMS is not only a surface process, but may be a volume effect as well. Ionization may precede ejection of molecular ions from multilayer samples of biomolecules.

The radial velocity distribution of secondary ions, ejected in a plasma desorption event, carries an important message about the ion formation mechanism. The correlation between directions of bombarding ion and sputtered particles may be used as a probe, allowing for better insight into the spatial as well as temporal sequence of the ionization/desorption events in PD in general [10]. We have recently studied the radial velocity distribution of $[M + nCs - (n - 1)H]^+$ where $n = 0, 1, 2$ for different peptides [10]. The fact that these distributions closely overlap demonstrates that both $[M + H]^+$ and $[M + Cs]^+$ ionic species for peptides with different masses are preferentially desorbed in a direction roughly perpendicular to the ion track, thus preserving a “memory” of the direction of the incident ion. Both alkali cation attachment and protonation in plasma desorption mass spectrometry are realized in a close spatial location and time interval within a similar distance from the ion track core. Thus the selvedge concept for “chemical ionization type” gas-phase alkali cation attachment in the case of PD [19,20] can be ruled out on the basis of these results. Simple kinematic considerations indicate that eventual post-desorption gas-phase collisions and ion–molecule association reactions would result in smearing and loss of the directional correlation of the resulting quasi-molecular ion adducts, which is not observed experimentally.

The possibility for the reverse process, i.e. the sputtering of clusters, followed by gas-phase uncluster decomposition of the type $[M + (n + 1)Cs -$

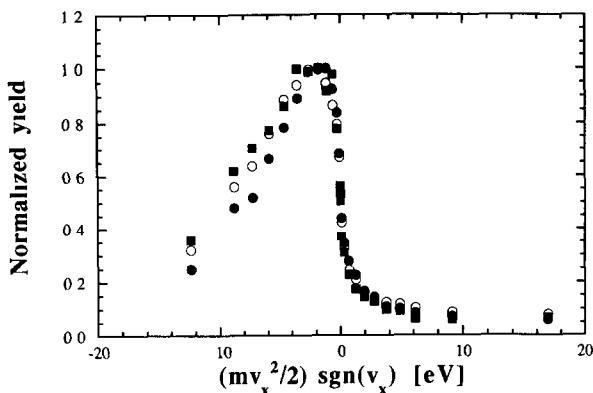


Fig 6 Radial energy distribution of leu-enkephalin molecular ions (data taken from ref 10)
 ●, $[M + H]^+$, ○, $[M + Cs]^+$, ■, $[M + 2Cs - H]^+$

$(n - 1)H]^+ \rightarrow [M + nCs - (n - 1)H]^+ + Cs$, where $n = 0, 1, 2$, may be discussed on the basis of the above observations [10]. A gas-phase uncluster decomposition would broaden the radial kinetic energy distribution for the $[M + H]^+$ and $[M + Cs]^+$ ions (compared with $[M + 2Cs - H]^+$) owing to isotropic translational energy release in that process. This should lead to an offset of the respective radial energy distributions, which is not experimentally observed (Fig. 6). A value of 0.15 eV for the released translational energy in the laboratory reference frame (resulting in a total broadening of 0.3 eV) would be within the limits of detection by the method employed. The full width at half-maximum (FWHM) of the radial energy distribution curves for the $[M + H]^+$ and $[M + Cs]^+$ leu-enkephalin ions is 8.07 ± 0.22 eV and 8.75 ± 0.17 eV respectively [10], a difference of -0.68 ± 0.28 eV. The sign of this difference ($-$) is opposite to that expected from translational energy release. While we could not find data in the literature for translational energy release in the case of uncluster decompositions we think that the above value (0.15 eV), although somewhat higher, may not be totally unrealistic in view of the small values of the excess internal energy [24] of the cation molecule complex.

Analytical models as well as molecular dynamics simulations [8,16,25] based on the shock wave concept predict similar radial velocities for ions ejected at similar distances from the ion track. The present results on the radial velocity distributions of radical molecular ions M^+ indicate that all different types of molecular ion—radical as well as even-electron quasi-molecular ions—are ejected within a similar distance from the ion track. While it is not possible in this experimental set-up to distinguish between preformed ions deposited on the target and species ionized at an early stage of the PD event, it is still certain that molecular ion formation precedes or

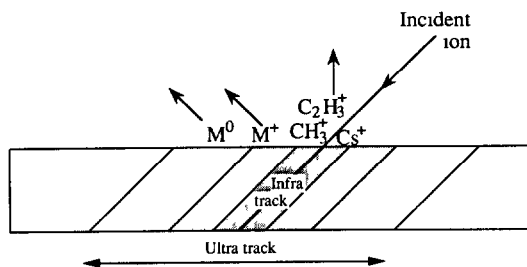


Fig 7 Schematic picture of the ion ejection process in PDMS M^+ indicates all types of molecular ion, even-electron as well as odd-electron ones

coincides with ejection into the gas phase. The radial velocity distribution of cluster ions (Fig 3 and ref 12) also points to direct ejection of “preformed” cluster ions, already existing in the solid, as opposed to gas-phase cluster formation.

The following qualitative model of ion formation emerges (Fig 7), based on the results presented here and on theoretical models for electronic sputtering of biomolecules [8,16,23,25]. The incoming ion deposits most of its energy in an ion track which is formed as a result of electronic excitation of the substrate molecules by the primary projectile and emission of δ electrons. Spatial regions with different energy densities, the infratrack and the ultratrack, axially symmetric to the incoming ion path, can be distinguished in the case of insulating materials (e.g. layers of biomolecules) as a target [25]. Molecular ion formation may take place in the ultratrack, in a region adjacent to the infratrack (Fig 6). Thus the ultratrack may be schematically subdivided into two regions, one where ionization occurs and a larger region from which ejection of intact neutral molecules takes place. Practically every molecule in the infratrack would be ionized and would have excess internal energy, thus dissociating to low mass fragments, owing to the higher energy density. The infratrack is the source of light mass fragment ions observed in the PDMS spectra. These light mass ions are thus sputtered in a direction uncorrelated with the direction of the incoming ion. A similar type of behaviour is predicted on the basis of thermal spike models of ion ejection [5,6]. Sputtering of different types of intact molecular ion from the ionization region in the ultratrack at an angle off the surface normal may be explained on the basis of the pressure pulse model [8]. While the directional correlation effect has been established for all types of singly and multiply charged molecular ions, we note that still there are no experimental results on the angular distribution of electromagnetically sputtered neutral biomolecules.

An obvious requirement for molecular ion formation is that the energy density in the ionization region should be higher than a threshold density,

depending on the ionization potential and the energy of intermolecular interactions of the biomolecules. The energy, transferred as an internal energy to the biomolecules, should not be large enough to cause excessive fragmentation. Results on radial velocity distributions of molecular ions of insulin in different charge states (protonated positive ions and deprotonated negative ions [11,13]) indicate that these ions are formed within the same distance from the ion track. Positive molecular ions from higher mass peptides (e.g. trypsin) in higher charge states are formed with higher probability closer to the ion track, in regions with higher energy density as compared with singly charged molecular ions [13]. Different types of reaction pathway may be advanced to explain formation of molecular ions within the ionization region. Direct ionization (as caused for example by the secondary δ electrons [25]) is a plausible mechanism. Another possibility is that the ionization step may be triggered by the pressure pulse. Fast solid state chemistry reactions may eventually take place in the region, perturbed by the shock wave. A documented effect of shock compression of dielectrics is the increase in their electrical conductivity, owing to a higher concentration of active particles (e.g. radicals, electrons, ions) [26]. This effect can facilitate molecular ion formation in the case of PD, including electron and proton transfer and cation attachment. A possible estimate of the contribution of the different effects can be obtained by comparison of the time scales involved. For instance, neutralization of the charged particle track takes place within 10^{-13} s. A rough estimate of the time scales involved in the ejection stage can be obtained from molecular dynamics simulations of the sputtering process for larger biomolecules [16]: the first molecules leave the surface at about 10^{-11} s, while the ejection yield saturates at about 10^{-10} s. Different phenomena could explain the lower yield of ejected molecular ions as compared with the yield of ejected intact neutral molecules [10]. These include the lower cross-section for different ionization processes on the surface or in the solid phase as well as a lower probability of survival of the molecular ions during the ejection stage (neutralization). A phenomenological description of the process of molecular ion formation and neutralization during shock wave ejection has been advanced [27] in order to incorporate the difference in the yield dependence on dE/dx (electronic stopping power) for neutrals and for molecular ions.

CONCLUSION

All types of molecular ion observed in PDMS of biomolecules—radical as well as even-electron quasi-molecular ions—are ejected from the target at an angle which is correlated with the angle of incidence of the incoming primary beam. This is in contrast to lower mass fragment ions, which display an angular distribution which is independent of the direction of the primary ion

These experimental results are interpreted in terms of the current pressure pulse model for electronic sputtering of biomolecules as an indication of ion ejection from two distinct spatial regions, axially symmetric about the primary ion track. The lower mass fragments are ejected from the infratrack region, where the higher energy density leads to ionization and subsequent fragmentation of the biomolecules. Intact molecular ions are sputtered from a region where the energy density of the propagating pressure pulse is high enough to cause their ejection but low enough to avoid their extensive fragmentation. While it is difficult to suggest a single ion formation mechanism, it can be asserted that molecular ions are either preformed or are ionized simultaneously with their ejection into the gas phase.

ACKNOWLEDGEMENTS

This work was supported by the Swedish Natural Sciences Research Council (NFR) and the Swedish National Board for Technical Development.

REFERENCES

- 1 B U R Sundqvist and R Macfarlane, *Mass Spectrom Rev*, 4 (1985) 421
- 2 R Macfarlane, J Hill and P Geno, in P Longevialle (Ed), *Advances in Mass Spectrometry*, Vol 11, Heyden, London, 1988, p 3
- 3 B U R Sundqvist, in P Longevialle (Ed), *Advances in Mass Spectrometry*, Vol 11, Heyden, 1988, p 363
- 4 B U R Sundqvist, *Nucl Instrum Methods Phys Res*, B48 (1990) 517
- 5 R Johnson, *Int J Mass Spectrom Ion Processes*, 78 (1987) 357
- 6 K Wien, *Radiat Eff Def Solids*, 109 (1989) 137
- 7 P Williams and B Sundqvist, *Phys Rev Lett*, 58 (1987) 1031
- 8 R Johnson, B U R Sundqvist, A Hedin and D Fenyo, *Phys Rev B*, 40 (1989) 49
- 9 A Hedin, P Håkansson, M Salehpour and B U R Sundqvist, *Phys Rev B*, 35 (1987) 7377
- 10 P Demirev, D Fenyo, P Håkansson and B U R Sundqvist, *Org Mass Spectrom*, 26 (1991) 471
- 11 D Fenyo, A Hedin, P Håkansson, R Johnson and B U R Sundqvist, in A Hedin, B U R Sundqvist and A Benninghoven (Eds), *Ion Formation from Organic Solids—IFOS V*, Wiley, Chichester, 1990, p 33
- 12 W Ens, B U R Sundqvist, P Håkansson, A Hedin and G Johnsson, *Phys Rev B*, 39 (1989) 763
- 13 D Fenyo, A Hedin, P Håkansson and B U R Sundqvist, *Int J Mass Spectrom Ion Processes*, 100 (1990) 63
- 14 P Håkansson, G Brinkmalm, J Kjellberg and B U R Sundqvist, *Proc 1st Int Conf Priority Trends in Scientific Instrumentation*, Leningrad, 1991, in press
- 15 R Mosshammer, R Matthaus, K Wien and G Bolbach, in A Hedin, B U R Sundqvist and A Benninghoven (Eds), *Ion Formation from Organic Solids—IFOS V*, Wiley, Chichester, 1990 p 17
- 16 D Fenyo, B U R Sundqvist, B Karlsson and R Johnson, *Phys Rev B*, 42 (1990) 1895

- 17 R Macfarlane, in G Waller and O Dermer (Eds), *Biochemical Applications of Mass Spectrometry*, Wiley, New York, 1980, p 1209
- 18 R Macfarlane, *Acc Chem Res* , 15 (1982) 268
- 19 S Pachuta and R G Cooks, *Chem Rev* , 87 (1987) 647
- 20 R J Cotter, *Anal Chem* , 60 (1988) 781A
- 21 R Macfarlane, B Wolf and D Bunk, in E Hilf and W Tuszynski (Eds), *PDMS of Large Non-volatile Molecules*, World Scientific, Singapore, 1990, p 10
- 22 G Save, P Håkansson, B U R Sundqvist, R Johnson, E Soderstrom, S Lindquist and J Berg, *Appl Phys Lett* , 51 (1987) 1379
- 23 S Della-Negra, J Depauw, H Joret, Y LeBeyec, I Bitensky, G Bolbach, R Galera and K Wien, *Nucl Instrum Methods Phys Res B*, 52 (1990) 121
- 24 P Burgers and J Holmes, *Rapid Commun Mass Spectrom* , 3 (1989) 279
- 25 A Hedın, P Håkansson, B U R Sundqvist and R Johnson, *Phys Rev B*, 31 (1985) 1780
- 26 V I Gol'danskii, E Ya Lantsburg and P A Yampol'skii, *JETP Lett* , 26 (1975) 166
- 27 I S Bitensky, A M Goldenberg and E S Parilis, in A Hedın, B U R Sundqvist and A Benninghoven (Eds), *Ion Formation from Organic Solids—IFOS V*, Wiley, Chichester, 1990, p 205